

Statistical Analysis of an Unbiased Plain Gradient Algorithm for a Constrained Adaptive IIR Notch Filter

R. Puchalard*, W. Loetwassana*, J. Koseeyaporn†, and P. Wardkein†

*Faculty of Engineering Mahanakorn University of Technology, Bangkok, Thailand

Tel: +66-2-988-3655, Fax: +66-2-988-4040, E-mail: rachu@mut.ac.th

† Faculty of Engineering King Mongkut's Institute of Technology Ladkrabang, Bangkok, Thailand

Abstract—Theoretical analysis of the unbiased plain gradient (UPG) algorithm for a constrained adaptive IIR notch filter (ANF) is presented in this paper. The difference equations for the convergence to the mean of the estimated parameter, estimation bias, and stability bound are derived. It is shown that the UPG provides bias smaller than that of the PG. Computer simulations have been treated to corroborate the theoretical analysis.

I. INTRODUCTION

It is well known that adaptive IIR notch filter (ANF) plays an important role in retrieving, detecting, or eliminating of narrow band signals or sinusoids corrupted by broad-band noise. Its applications are found in radar, sonar, communication system, biomedical engineering, and so on [1]-[6].

Recently, Puchalard *et al.* has proposed the unbiased plain gradient (UPG) algorithm for a constrained ANF [1]. It was shown that the UPG provided low bias for all values of ρ , signal to noise ratio (SNR), and signal frequency ω_0 compared with the PG algorithm [6]. However, only simulation results were conducted to corroborate the performance of the UPG in [1] but the theoretical analysis of the UPG has not yet been studied.

Therefore, the theoretical analysis of the UPG is presented in this paper. The difference equations for the convergence to the mean of the filter parameter, bias, and stability bound are derived. Additionally, the computer simulations are conducted to confirm the effectiveness of the UPG algorithm.

This paper is organized as follows. Section 2 provides the history of the constrained ANF and the UPG. The analytical technique of the UPG is introduced in section 3. Results and discussions are provided in section 4 where section 5 is for the conclusion of this work.

II. ADAPTIVE IIR NOTCH FILTER AND THE UPG

In this section, the adaptive IIR notch filter with constrained poles and zeros (ANF) and the unbiased plain gradient (UPG) adaptive algorithm are briefly discussed. For the ANF, its transfer function is given by

$$H(z) = \frac{1 + az^{-1} + z^{-2}}{1 + \rho az^{-1} + \rho^2 z^{-2}} \quad (1)$$

where a ($-2 < a < 2$) is the filter parameter to be adapted, ρ ($0 \ll \rho < 1$) is a pole radius controlling the notch

bandwidth. Referring to [1], the UPG algorithm that adjusts the filter parameter a can be described as

$$a(k+1) = a(k) - \mu e(k)(g(k) - Ca(k)x(k)) \quad (2)$$

where $C = \rho(1-\rho)/(1+\rho)$, μ is the step size parameter controlling the speed of convergence, which is generally positive constant real number, and $e(k)$ is the notch output or error signal which is given by

$$e(k) = x(k) + ax(k-1) + x(k-2) - \rho ae(k-1) - \rho^2 e(k-2). \quad (3)$$

It is noted that $g(k)$ is the gradient of $e(k)$ with respect to a at $a = a(k)$, which is

$$g(k) \approx x(k-1) - \rho e(k-1). \quad (4)$$

It is found that $g(k)$ is produced by $G(z)$ which is given by [6]

$$G(z) = (1-\rho)z^{-1} \frac{1-\rho z^{-2}}{1+\rho az^{-1} + \rho^2 z^{-2}}. \quad (5)$$

From (3), $x(k)$ is the input signal of the form

$$x(k) = A \cos(\omega_0 k + \theta) + v(k) \quad (6)$$

where A is the signal amplitude, ω_0 is the signal frequency, θ is the signal phase which is uniformly distributed over $[0, 2\pi)$ and $v(k)$ is a zero mean white Gaussian noise with variance σ_v^2 .

III. CONVERGENCE BEHAVIOR AND BIAS ANALYSIS

In this section, convergent behavior and bias of the UPG at the steady state are addressed. At steady-state, equations (1) and (5) can be respectively rewritten as [6]

$$H(e^{j\omega_0}) \approx \frac{\delta_a}{a_0(\rho-1) + (\rho^2-1)e^{-j\omega_0}} - \frac{\rho\delta_a^2}{\{a_0(\rho-1) + (\rho^2-1)e^{-j\omega_0}\}^2} \quad (7)$$

$$G(e^{j\omega_0}) \approx e^{-j\omega_0} - \frac{\rho\delta_a}{a_0(\rho-1) + (\rho^2-1)e^{-j\omega_0}} + \frac{\rho^2\delta_a^2 e^{-j\omega_0}}{\{a_0(\rho-1) + (\rho^2-1)e^{-j\omega_0}\}^2} \quad (8)$$

where $\delta_a = \hat{a} - a_0$ is the estimation error and \hat{a} is an estimate of a_0 . It is noted that at time k , a is replaced by $a(k)$. The corresponding output signals generated by (7) and (8) can be expressed respectively as follows:

$$e_s(k) = AB\delta_a(k) \cos(\omega_0 k + \theta - \phi) - \rho AB^2 \delta_a^2(k) \cos(\omega_0 k + \theta - 2\phi) + v_1(k) \quad (9)$$

$$g_s(k) = A \cos(\omega_0 k + \theta - \omega_0) - \rho AB\delta_a(k) \cos(\omega_0 k + \theta - \omega_0 - \phi) + \rho^2 AB^2 \delta_a^2(k) \cos(\omega_0 k + \theta - \omega_0 - 2\phi) + v_2(k). \quad (10)$$

From (9) and (10), B and ϕ are magnitude and phase of the first term (without δ_a) on the right-handed side (RHS) of (7), which are shown respectively as

$$B = \frac{1}{(1-\rho)\sqrt{(1+\rho)^2 - 4\rho \cos^2 \omega_0}} \quad (11)$$

$$\phi = \begin{cases} \phi_0, & \omega_0 \leq \pi/2 \\ \pi + \phi_0, & \omega_0 > \pi/2 \end{cases} \quad (12)$$

where

$$\phi_0 = \tan^{-1} \frac{(1+\rho) \sin \omega_0}{(1-\rho) \cos \omega_0}. \quad (13)$$

In addition, $v_1(k)$ and $v_2(k)$ are assumed to be zero-mean Gaussian noises at the output of (1) and (5) excited with $v(k)$, respectively. The correlation between $v_1(k)$ and $v_2(k)$ denoted as R_{12} is computed by [6]

$$R_{12} = E[v_1(k)v_2(k)] = \frac{-2\rho(1-\rho)\cos\omega_0\sigma_v^2}{1+\rho} - \frac{2(1-\rho)^3\cos\omega_0}{1+\rho\rho^4-2\rho^2\cos 2\omega_0+1}\sigma_v^2. \quad (14)$$

The convergent behavior of the UPG can be computed by substituting (6), (9), and (10) into (2) and taking the expectation of the result, which yields

$$E[a(k+1)] = E[a(k)] - \mu E[e_s(k)g_s(k)] + \mu CE[a(k)e_s(k)x(k)] = E[a(k)] - \mu M_1(k) + \mu Ca_0 M_2(k) \quad (15)$$

where $E[\cdot]$ is an expectation operator, $M_1(k) = E[e_s(k)g_s(k)]$, and $M_2(k) = E[e_s(k)x(k)]$. Note that the coefficient $a(k)$ involved in the last term on the RHS of (15) is replaced with a_0 for simplicity. The computations of $M_1(k)$ and $M_2(k)$ related to signal only can be determined as follows:

$$\begin{aligned} M_1(k) |_{\text{signal}} &= E[\{AB\delta_a(k) \cos(\omega_0 k + \theta - \phi) \\ &\quad - \rho AB^2 \delta_a^2(k) \cos(\omega_0 k + \theta - 2\phi)\} \\ &\quad \times \{A \cos(\omega_0 k + \theta - \omega_0) \\ &\quad - \rho AB\delta_a(k) \cos(\omega_0 k + \theta - \omega_0 - \phi) \\ &\quad + \rho^2 AB^2 \delta_a^2(k) \cos(\omega_0 k + \theta - \omega_0 - 2\phi)\}] \\ &\approx \frac{1}{2} A^2 B \cos(\omega_0 - \phi) E[a(k)] \\ &\quad - \frac{1}{2} A^2 B a_0 \cos(\omega_0 - \phi) \\ &= \psi_{11} E[a(k)] - a_0 \psi_{11} \end{aligned} \quad (16)$$

$$\begin{aligned} M_2(k) |_{\text{signal}} &= E[\{AB\delta_a(k) \cos(\omega_0 k + \theta - \phi) \\ &\quad - \rho AB^2 \delta_a^2(k) \cos(\omega_0 k + \theta - 2\phi)\} \\ &\quad \times \{A \cos(\omega_0 k + \theta)\}] \\ &\approx \frac{1}{2} A^2 B \cos(\phi) E[a(k)] \\ &\quad - \frac{1}{2} A^2 B a_0 \cos(\phi) \\ &= \psi_{12} E[a(k)] - a_0 \psi_{12} \end{aligned} \quad (17)$$

where

$$\psi_{11} = \frac{1}{2} A^2 B \cos(\omega_0 - \phi) \quad (18)$$

$$\psi_{12} = \frac{1}{2} A^2 B \cos(\phi). \quad (19)$$

Furthermore, the computations related to noise only can be estimated as

$$M_1(k) |_{\text{noise}} = E[v_1(k)v_2(k)] = R_{12} = (14) \quad (20)$$

$$\begin{aligned} M_2(k) |_{\text{noise}} &= E[v(k)v_1(k)] \\ &= \frac{\sigma_v^2}{2\pi j} \oint H(z)z^{-1} dz \\ &= \sigma_v^2. \end{aligned} \quad (21)$$

By using (16)-(21) and the relation $\delta_a(k) = a(k) - a_0$ into (15), it results in

$$\begin{aligned}
 E[a(k+1)] &= E[a(k)] \\
 &\quad - \mu(\psi_{11}E[a(k)] - a_0\psi_{11}) \\
 &\quad + \mu Ca_0(\psi_{12}E[a(k)] - a_0\psi_{12}) \\
 &\quad - \mu(R_{1,2} - Ca_0\sigma_v^2). \tag{22}
 \end{aligned}$$

From (22), it is observed that when $\rho \rightarrow 1$, $R_{1,2}|_{\rho \rightarrow 1} \approx \frac{-2\rho(1-\rho)\cos\omega_0}{1+\rho}\sigma_v^2 = Ca_0\sigma_v^2$, and (22) can be simplified to be

$$\begin{aligned}
 E[a(k+1)] &= (1 - \mu\psi_{11} + \mu Ca_0\psi_{12})E[a(k)] \\
 &\quad + \mu(a_0\psi_{11} - Ca_0^2\psi_{12}). \tag{23}
 \end{aligned}$$

(23) is the difference equation for the convergence to the mean of the parameter $a(k)$, and can be used to study the convergence behavior of the UPG algorithm. It is noted that (16) and (17) are obtained by omitting the terms $\delta_a^m, m > 2$. These terms can be neglected when μ is small. By assuming that $E[a(k+1)]_{k \rightarrow \infty} = E[a(k)]_{k \rightarrow \infty} = E[a(\infty)]$, (23) becomes

$$E[a(\infty)] = \frac{a_0(\psi_{11} - Ca_0\psi_{12})}{(\psi_{11} - Ca_0\psi_{12})} = a_0. \tag{24}$$

(24) is the closed-form expression of the parameter estimate of the UPG at the steady state. It can be seen that the UPG provides unbiased estimate of the parameter $a(k)$ when ρ and μ are sufficient large and small, respectively. However, it is found in the computer simulation results that the UPG provides low bias compared with the conventional PG even with small and large value of ρ and μ , respectively. Similarly from (23), it is easy to obtain the difference equation for the convergence to the mean of bias of the UPG, which is

$$E[\delta_a(k+1)] = (1 - \mu\{\psi_{11} - Ca_0\psi_{12}\})E[\delta_a(k)]. \tag{25}$$

It is found that the closed-form expression for the bias in the steady state is infeasible because (25) is nonlinear. Hence, many solutions of (25) can exist, however, the desired solution is $E[\delta_a(k)] = 0$, which the solution at stationary point of (25). As a result, after the convergence of the UPG, it is unbiased estimator.

IV. COARSE STABILITY BOUND

The coarse stability bound of the UPG can be obtained by examining (25). It is found that this equation will be stable if the following condition is satisfied:

$$|1 - \mu\{\psi_{11} - Ca_0\psi_{12}\}| < 1. \tag{26}$$

From (26), the coarse stability for step size μ will be

$$0 < \mu < \frac{2}{\psi_{11} - Ca_0\psi_{12}}. \tag{27}$$

The bound of step size shown in (27) is a coarse stability because it is derived from (25), which is the approximation of the true bias. However, a coarse stability is useful in practice, especially when the true stability is infeasible.

V. RESULTS

In this section, the computer simulations have been conducted to corroborate the theoretical analyses. In order to obtain the estimated parameter $E[a(k)]$ and estimation bias $E[\delta_a(k)]$ from simulations, the number of iteration is allowed to be large enough so that the simulations reach the steady-state. The noisy sinusoidal signals of difference phases and noise sequences are applied to the tested filter. The results of estimating are ensemble averaged to produce the simulated values. Fig. 1 (a) and (b) shows the trajectories of $E[a(k)]$ and $E[\delta_a(k)]$, respectively, for small value of ρ and large value of μ (fast adaptation). It is seen that the theoretical values of both $E[a(k)]$ and $E[\delta_a(k)]$ show large differences from their simulated results. This fact is not surprised because the UPG was developed based on assuming that the pole radius must be close to one, $\rho \rightarrow 1$ [1]. The difference between theory and simulation is due to the omitting of the terms $\delta_a^m, m > 2$, which implies that the theory is invalid for this case. Nevertheless, the bias producing by the UPG is smaller than that of the conventional PG. Fig. 2 (a) and (b) represents the trajectories of $E[a(k)]$ and $E[\delta_a(k)]$, respectively, for large value of ρ and large value of μ (fast adaptation). As can be seen in this figure, the theoretical shows difference the simulation only in the region of transient. This is due to the neglecting the terms $\delta_a^m, m > 2$. In steady state region ($k > 1000$), the theoretical can track simulation well. Moreover, the bias producing by the UPG is lower than that of the PG. For slow adaptation in which small values of μ and ρ are employed, which is shown in Fig. 3 (a) and (b) for $E[a(k)]$ and $E[\delta_a(k)]$, respectively. The theoretical values of UPG still show difference from their simulations. On the other hand, when large value of ρ is employed, which is shown in Fig. 4 (a) and (b), the theoretical values are accordant with the simulated results in steady state region ($k > 100000$). However, the theoretical value and simulation result within the transient state are still different. This is due to the approximation of calculation. For the PG, it still provides large bias compared with that of the UPG although large value of ρ is employed. Finally, Fig. 5 demonstrates the stability bound for step size parameter with respect to pole radius ρ . Although the theory and simulation results show relatively differences, the theoretical stability bound provides a similar tendency of decreasing with the increment of ρ . As has been discussed, the UPG is the conditional unbiased estimator where the pole radius must be close to one.

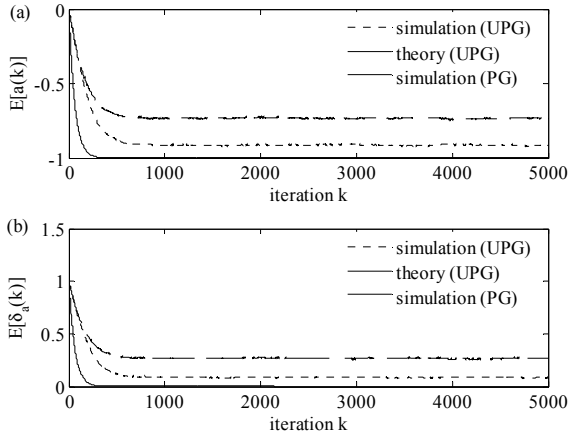


Fig. 1. Trajectories of $E[a(k)]$ and $E[\delta_a(k)]$ obtainable by the UPG and PG for $A = \sqrt{2}$, $\omega_0 = \pi/3$, $\theta = \pi/6$, $\mu = 0.01$, $\rho = 0.5$, $\sigma_v^2 = 1$, and 200 independent runs: (a) $E[a(k)]$ (b) $E[\delta_a(k)]$.

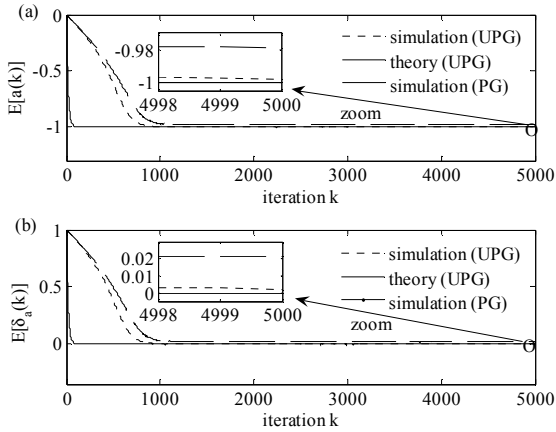


Fig. 2. Trajectories of $E[a(k)]$ and $E[\delta_a(k)]$ obtainable by the UPG and PG for $A = \sqrt{2}$, $\omega_0 = \pi/3$, $\theta = \pi/6$, $\mu = 0.01$, $\rho = 0.9$, $\sigma_v^2 = 1$, and 200 independent runs: (a) $E[a(k)]$ (b) $E[\delta_a(k)]$.

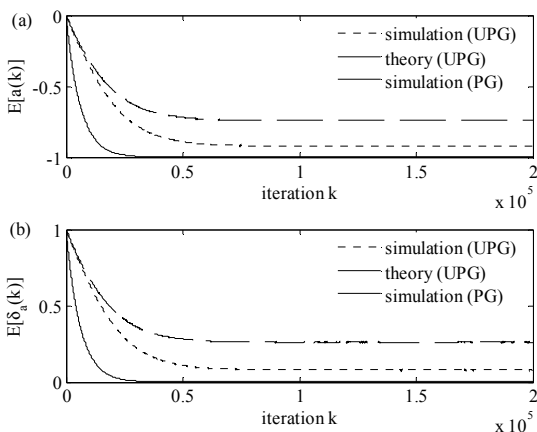


Fig. 3. Trajectories of $E[a(k)]$ and $E[\delta_a(k)]$ obtainable by the UPG and PG for $A = \sqrt{2}$, $\omega_0 = \pi/3$, $\theta = \pi/6$, $\mu = 0.0001$, $\rho = 0.5$, $\sigma_v^2 = 1$, and 200 independent runs: (a) $E[a(k)]$ (b) $E[\delta_a(k)]$.

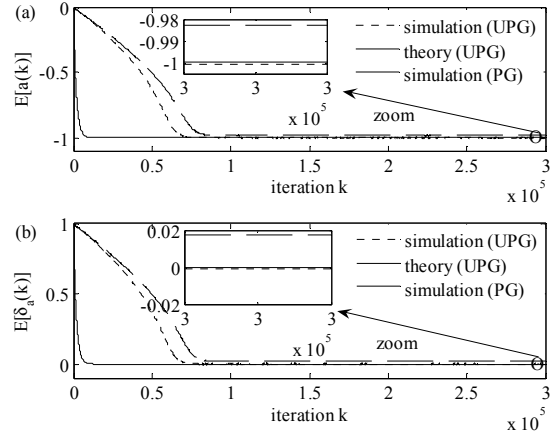


Fig. 4. Trajectories of $E[a(k)]$ and $E[\delta_a(k)]$ obtainable by the UPG and PG for $A = \sqrt{2}$, $\omega_0 = \pi/3$, $\theta = \pi/6$, $\mu = 0.0001$, $\rho = 0.9$, $\sigma_v^2 = 1$, and 200 independent runs: (a) $E[a(k)]$ (b) $E[\delta_a(k)]$.

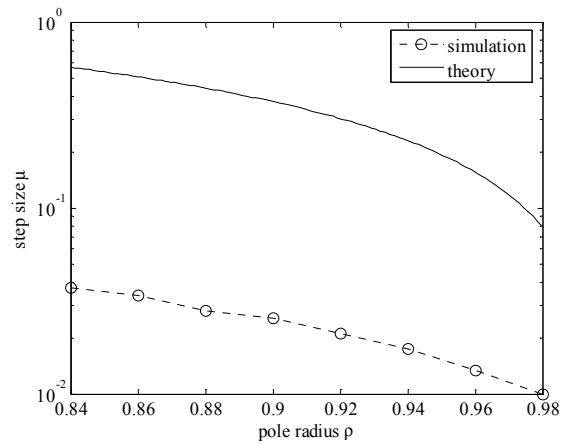


Fig. 5. Stability bound of the UPG versus pole radius ρ for $A = \sqrt{2}$, $\theta = \pi/6$, $\sigma_v^2 = 0.1$, $\omega_0 = \pi/3$, 100 independent runs.

VI. CONCLUSIONS

The analysis of the UPG for the ANF with constrained poles and zeros is presented in this work. The convergence behavior of the estimated parameter, estimation bias, and stability bound are carried out. It has been shown that the UPG is unbiased estimator only when $\rho \rightarrow 1$. Nevertheless, the UPG provides bias smaller than that of the PG for all values of ρ and μ . For the mean square error analysis of the UPG which is also an interesting topic will be further studied in the future work.

REFERENCES

- [1] R. Panchalard, A. Lorsawatsiri, W. Loetwassana, J. Koseeyaporn, P. Wardkein, and A. Roesabutr, "Unbiased plain gradient algorithm for adaptive IIR notch filter with constrained poles and zeros," in *IEEE Proceeding TENCON*, Oct. 2007.
- [2] K. Martin and M. T. Sun, "Adaptive filters suitable for real-time spectral analysis," *IEEE Trans. Circuits Syst.*, vol. 33, no. 2, pp. 281-229, Feb. 1986.
- [3] T. Kwan and K. Martin, "Adaptive detection and enhancement of multiple sinusoids using a cascade IIR filter," *IEEE Trans, Circuits Syst.*, vol.3., no. 7, pp. 937-947, Jul. 1989.

- [4] N. I. Cho, C. H. Choi, and S. U. Lee, "Adaptive line enhancement by using an IIR lattice notch filter," *IEEE Trans. Acoust., Speech, Signal Process.*, vol. 37, no. 4, pp. 585-589, Apr. 1989.
- [5] J. F. Chicharo and t. S. Ng, "Gradient-based adaptive IIR notch filtering for frequency estimation," *IEEE Trans. Acoust., Speech, Signal Process.*, vol. 38, no. 5, pp. 769-777, Sep. 1990.
- [6] Y. Xiao, Y. Takeshita, and K. Shida, "Steady-State analysis of a plain gradient algorithm for a second-order adaptive IIR notch filter with constrained poles and zeros," *IEEE Trans. Circuits Syst. II.*, vol. 48, pp. 733-740, Jul. 2001.